FTIR Analysis of the Interaction of Azide with Horse Heart Myoglobin Variants†

Ralf Bogumil,‡,§ Christie L. Hunter,‡,∥ Robert Maurus,‡,⊥ Hai-Lun Tang,‡ Hung Lee,# Emma Lloyd,‡ Gary D. Brayer,‡ Michael Smith,‡,○ and A. Grant Mauk*,‡

Department of Biochemistry and Molecular Biology and Protein Engineering Network of Centres of Excellence, University of British Columbia, Vancouver, British Columbia V6T 1Z3, Canada, and Department of Environmental Biology, University of Guelph, Guelph, Ontario N1G 2W1, Canada

Received December 21, 1993; Revised Manuscript Received March 22, 1994®

ABSTRACT: The interaction of azide with variants of horse heart myoglobin (Mb) has been characterized by Fourier transform infrared (FTIR), electron paramagnetic resonance (EPR), and UV–VIS absorption spectroscopy and by molecular modeling calculations. Distal histidine variants (His64Thr, His64Ile, His64Lys) and charged surface variants (Val67Arg, Lys45Glu, Lys45Glu/Lys63Glu) were included in this study. All variants, with the exception of Val67Arg, have a lower azide affinity than the wild-type protein. Analysis of the temperature dependence of the FTIR spectra (277–313 K) revealed that the wild-type protein and all variants exhibit a high-spin/low-spin equilibrium. Introduction of positively charged amino acid residues shifts ν_{max} for the low-spin form to higher energy while negatively charged residues shifted this maximum to lower energy. The low azide binding affinity exhibited by the His64Thr and His64Ile variants is accompanied by a shift of the ν_{max} for the low-spin infrared band to lower energy and by a significant increase in the corresponding half-bandwidths. This observation indicates greater mobility of the bound azide ligand in these variants. The His64Lys variant exhibits two infrared bands attributable to low-spin forms that are assigned to two different conformations of the lysyl residue. In one conformation, the lysine is proposed to form a hydrogen bond with the bound azide similar to that proposed to occur between the distal histidine and bound azide, and in the other conformation no interaction occurs.

In recent years, site-directed mutagenesis has been used to examine the role of critical amino acid residues in the active sites of several mammalian myoglobins (Mbs) through both spectroscopic and structural studies (Egeberg et al., 1990; Adachi et al., 1992, 1993; Ikeda-Saito et al., 1992). The modulating role of the distal histidyl residue, His64, in ligand binding has received particular attention through analysis of variants in which this residue has been replaced by a variety of amino acid residues (Springer et al., 1989; Rohlfs et al., 1990; Carver et al., 1990; Cutruzzola et al., 1991; Ikeda-Saito et al., 1992; Biram et al., 1993; Quillin et al., 1993). Several studies have assessed the effects of distal histidine substitutions on binding of carbon monoxide to ferromyoglobin through the correlation of results obtained by Fourier transform infrared (FTIR) spectroscopy and ligand binding kinetics (Braunstein et al., 1988; Balasubramanian et al., 1993). Although the effects of some active-site substitutions on azide binding affinity to ferrimyoglobin variants have been studied (Ikeda-Saito et al., 1992; Cutrozzola et al., 1991; Biram et al., 1993), the corresponding spectroscopic analyses of these MbN_3 complexes have not been reported.

$MetMbN_3$ and $metHbN_3$ complexes both exhibit a low-spin ground state and an observable spin equilibrium near room temperature (Iizuka & Kotani, 1968, 1969a,b). This spin equilibrium has been studied by magnetic susceptibility measurements (Beetlestone & George, 1964; Iizuka & Kotani, 1968, 1969a) and by infrared (Alben & Fager, 1972) and resonance Raman (Tsubaki et al., 1981) spectroscopy. Recently, MbN_3, MbCN, and MbC_2H_5SH complexes were studied by electron spin-echo envelope modulation spectroscopy (Magliozzo & Peisach, 1993). For the MbN_3 complex, this study revealed that the origin of the weak ligand field associated with the high-spin/low-spin equilibrium is a weakened σ-bond between the proximal histidine and the ferric ion.

The infrared spectra of wild-type MbN_3 complexes were first reported by McCoy and Caughey (1970). These authors identified infrared bands at 2023 and 2046 cm^{-1} and assigned them to the antisymmetric stretch of bound azide. Their assignments of lower frequencies to low-spin species and higher frequencies to high-spin species were confirmed by Alben and Fager (1972), who showed that the relative intensities of the two infrared bands exhibited a temperature dependence expected for a thermal spin equilibrium. The estimated equilibrium constant K_s = [N_3](low-spin)/[N_3](high-spin) was different for hemoglobin and myoglobin derivatives and varied with the origin of the protein.

In this report, FTIR spectra, EPR spectra, and equilibrium binding constants of MbN_3 complexes are reported for several variants of horse heart myoglobin with changes in or near the distal heme pocket. In the variants studied, the distal histidine (His64) was substituted with lysine (His64Lys), isoleucine (His64Ile), and threonine (His64Thr) because this residue is known to be important for ligand binding, and large differences were observed in the FTIR spectra of CO-bound Mb variants (Balusubramanian et al., 1993). In addition, the effects of charged surface residues near the heme pocket on ligand binding were assessed by consideration of variants in which

† This work and the purchase of the EPR spectrometer and computational hardware and software were supported by the Protein Engineering Network of Centres of Excellence. The FTIR spectrometer was obtained with funds provided by the B.C. Health Care Research Foundation.

‡ University of British Columbia.

§ Recipient of a postdoctoral fellowship from the Deutsche Forschungsgemeinschaft.

∥ Recipient of a UBC I. W. Killam Graduate Studentship.

⊥ Recipient of an MRC Studentship.

University of Guelph.

○ MRC Career Investigator.

® Abstract published in *Advance ACS Abstracts,* May 1, 1994.

0006-2960/94/0433-7600$04.50/0

positively (Val67Arg) and negatively (Lys45Glu; Lys45Glu/Lys63Glu) charged amino acid residues are introduced at different distances from the azide binding site. Examination of the structure and ligand binding behavior relationships of these variants was performed by combining spectroscopic results with computer-aided molecular modeling.

MATERIALS AND METHODS

Protein Preparation. The preparation and purification of recombinant horse heart (HH) Mb have been described elsewhere (Guillemette et al., 1991). Commercial horse heart myoglobin was purchased from Sigma, and sodium azide (reagent grade) was from BDH.

Determination of the Equilibrium Constant of MbN_3 Complexes. The affinity of wild-type and variant ferrimyoglobins for azide was measured by spectrophotometric titration. A known amount of azide was added to the Mb solution (ca. 10 μM, 0.1 M sodium phosphate buffer, pH 7.0, 20 °C) in a 1-mL cuvette, and the decrease in intensity of the Soret band was measured. Spectra were recorded with a Cary 219 spectrophotometer interfaced to a microcomputer (OLIS, Bogart, Georgia) and fitted with a thermostated, circulating water bath (Lauda Model RS3). Each titration curve was comprised of 10–15 points. The volume of azide solution added (2 mM, 10 mM, 200 mM, or 1 M, depending on the protein concerned) was kept to a minimum (0.5–2 μL/addition) so sample dilution was not a factor. The equilibrium dissociation constants for the variants with greater binding affinity (wild-type, Val67Arg, His64Lys, and Lys45Glu) were calculated according to eq 1 (Ikeda-Saito et al., 1992). Fractional

$$[MbN_3]/[Mb]_{tot} = [N_3^-]_{free}/(K_d^{app} + [N_3^-]_{free}) \quad (1)$$

saturation, $[MbN_3]/[Mb]_{tot}$, was determined from the absorbance change caused by azide binding divided by the absorbance change at azide saturation. The variants with significantly lower binding constants, His64Thr and His64Ile, were not titrated to saturation as concentrations of azide were required that would have resulted in significant increases in ionic strength. Assuming that $[N_3^-]_{free} = [N_3^-]_{tot}$, an alternative equation (eq 2) can be derived. In this equation,

$$Abs = (K_d^{app}Abs_i + [N_3^-]_{tot}Abs_f)/(K_d^{app} + [N_3^-]_{tot}) \quad (2)$$

Abs_i is the initial absorption of the Mb solution in the absence of azide and Abs_f is the final absorption at azide saturation. Use of this relationship avoids the necessity of achieving complete saturation of the protein with ligand. Equilibrium binding data were fitted to eq 1 or 2 with the program MINSQ (MicroMath, Salt Lake City, UT).

FTIR Spectroscopy. FTIR spectra were recorded at 2-cm^{-1} resolution with a Perkin-Elmer System 2000 FTIR spectrometer equipped with a liquid nitrogen cooled mercury cadmium telluride detector. Concentrated Mb solutions (4–7 mM) in 100 mM potassium phosphate, pH 7.0, were mixed with small amounts of a 40 mM sodium azide solution in the same buffer. A slight excess of myoglobin was used to minimize bands attributable to free azide. The protein solution was loaded into a cell with CaF_2 windows and a 0.05-mm spacer and placed into a water-jacketed cell holder (Specac, Inc.) connected to a thermostated, circulating water bath (Lauda Model RS3). Absorption spectra in the range 1900–2100 cm^{-1} were obtained from the difference between the spectra of the MbN_3 complexes and the spectrum of wild-type Mb without azide. The infrared spectrum of Mb in the absence of azide (minus the buffer spectrum) does not exhibit any significant bands over this range. An average of 250 scans was used for each spectrum.

Infrared absorption spectra were fitted with a linear combination of both Gaussian and Lorentzian line shapes using the curvefit function of the program Grams/386 (Galactic Industries). The linear combination of Gaussian and Lorentzian line shapes usually produced better fits than the use of pure Gaussian or Lorentzian functions. The minimum number of bands required to produce acceptable residuals plots (experimental curve minus theoretical curve, as illustrated) was used for analysis of spectra. The ν_{max} and the line width of the absorption band of the unbound azide ion were fixed during the fitting process for the MbN_3 spectra in which the concentration of unbound azide was significant.

EPR Spectroscopy. Ferrimyoglobin samples in potassium phosphate buffer (pH 7.0) were mixed with a concentrated sodium azide solution in the same buffer to give a final concentration of 0.2 M azide and 1 mM ferri-Mb. EPR spectra were obtained at X-band frequencies (ca. 9.5 GHz) using a Bruker ESP 300E spectrometer equipped with an Oxford Instruments liquid helium cryostat and an Oxford Instruments ITC4 temperature controller. The experimental conditions used were 10 K, 0.63-mW microwave power, 9.45-GHz microwave frequency, 100-kHz modulation frequency, and 1-mT modulation amplitude.

Molecular Modeling. All energy minimizations were performed on a model system based on the structure of recombinant wild-type horse heart Mb. This structure has been determined to 1.8 Å resolution (Maurus et al., unpublished results) and found to be identical to that of myoglobin isolated from horse heart (Evans & Brayer, 1988, 1990). The starting models for variant proteins were constructed by substituting exchanged residues into the wild-type protein structure. Water molecules identified in the original structure determination process were added to all models, and the overall protein–water model was further surrounded by a 8 Å thick layer of solvent water. Energy minimization of all models was carried out with the program Discover (Biosym Technologies, San Diego, CA). Potential energy parameters and partial charges were assigned on the basis of the consistence valence force field (CVFF) (Biosym Technologies). No cross-terms were used in the potential energy functions, and a simple harmonic potential was chosen for bond stretching terms. The charge states of ionizable groups were assumed to be those present at pH 7.0. The effect of substituting experimentally determined values for pK_as of histidine residues (Cocco et al., 1992) was also evaluated. All hydrogen atoms were explicitly represented, and a dielectric constant of 1.0 was used in all calculations. A cutoff distance of 10 Å was used for nonbonding interactions with a switching function applied over the last 1.5 Å of the cutoff distance.

Energy minimizations were carried out in several steps designed to preserve the experimentally determined structure of the protein as much as possible. In the initial stage, the solvent around the protein molecule was allowed to relax around the fixed protein molecule. All side chain atoms, including those of substituted residues, were then included in the minimization, keeping the main chain atoms frozen. In the final stage, the entire assembly was allowed to move, with the minimization proceeding by the conjugate gradient algorithm until convergence (highest derivative <0.01 kcal/mol Å).

Table 1: Equilibrium Dissociation Constants for Azide Binding to Wild-Type and Variants of MetMb (0.1 M Sodium Phosphate Buffer, pH 7.0, 20 °C)

protein	K_d^{app} (μM)	relative to wild-type
wild-type	20 ± 1	1
commercial wild-type	26.0 ± 0.5	1.3
Lys45Glu	99 ± 3	5
Lys45Glu/Lys63Glu	280 ± 10	14
Val67Arg	4.0 ± 0.5	0.2
His64Thr	440 ± 20	20
His64Lys	74 ± 1	3.7
His64Ile	4200 ± 200	209

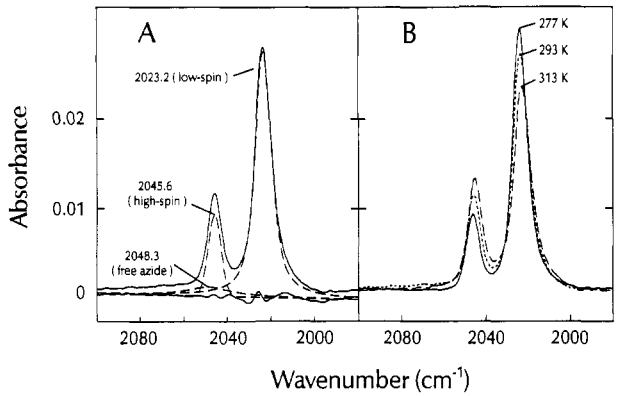

FIGURE 1: Infrared spectra of the wild-type metMbN_3 complex (5.0 mM Mb, 4 mM azide, pH 7.0, 293 K). (A) Infrared spectrum of the recombinant wild-type MbN_3 complex. Experimental spectrum, upper solid line; absorption bands identified from curve-fitting procedure, dashed lines; residual (experimental spectrum minus sum of fitted absorption bands), lower solid line. (B) Infrared spectra of recombinant wild-type MbN_3 collected as a function of temperature.

RESULTS

Ligand Binding Parameters. The binding of azide to all of the ferrimyoglobin variants studied here conforms to a single equilibrium with a binding stoichiometry of 1:1. The results are summarized in Table 1. The dissociation constant determined for recombinant wild-type Mb (20 μM) agrees well with that for horse heart myoglobin obtained from a commercial source (Sigma) (26 μM) and with values reported for human (25 μM; Ikeda-Saito et al., 1992) and sperm whale myoglobin (27 μM; Cutruzzola et al., 1991). The affinity of azide binding to the variants studied here decreases in the following order: Val67Arg > wild-type > His64Lys > Lys45Glu > Lys45Glu/Lys63Glu > His64Thr > His64Ile. The absorption spectra of the azide complexes of the Mb variants are essentially identical to that of the complex formed by azide with wild-type Mb.

FTIR Spectra. Figure 1A shows the FTIR spectrum of the recombinant wild-type MbN_3 complex at 293 K in the region of the asymmetric stretching vibration of the azide ion. The two bands at 2023.2 and 2045.6 cm^{-1} can be assigned to the low-spin and the high-spin form of bound azide, respectively. The broad band at 2048.3 cm^{-1} is attributable to a small amount of unbound azide. The values for the ν_{max} and half-bandwidth are nearly identical to the values obtained with a sample of commercial horse heart Mb (2023.4, 2045.9 cm^{-1}) and to the values of 2023.4 and 2045.8 cm^{-1} reported by Alben and Fager (1972).

The temperature dependence of the infrared absorption spectrum observed for recombinant wild-type Mb is shown in Figure 1B. The absorption band of the high-spin form increases in intensity with increasing temperature concomitant with a corresponding decrease in intensity of the absorption band for the low-spin form, as expected for a temperature-dependent spin-state equilibrium with a low-spin ground state. The values of the band maxima and half-bandwidth obtained by curve-fitting for recombinant wild-type myoglobin and the distal pocket mutants are listed in Table 2. In most variants, the estimated errors in ν_{max} are in the range of ±0.1 cm^{-1} and for the half-bandwidth ±0.2 cm^{-1}. In the case of the distal histidine variants where the half-bandwidths are larger and significant amounts of free azide are present, the errors of this analysis are greater (~0.5–1 cm^{-1}).

Table 2: Absorption Maxima Derived by Curve-Fitting Analysis for MbN_3 Derivatives

	ν (cm^{-1})			$\Delta\nu_{1/2}$ (cm^{-1})		
sample	277 K	293 K	313 K	277 K	293 K	313 K
wild-type metMb						
low-spin	2023.7	2023.2	2022.2	8.3	8.7	9.4
high-spin	2046.1	2045.6	2045.2	7.3	7.0	7.4
Lys45Glu						
low-spin	2023.3	2022.8	2022.2	8.3	8.8	9.4
high-spin	2046	2045.6	2045.2	7.1	7.5	8
Lys45Glu/Lys63Glu						
low-spin	2023.3	2022.8	2022.2	8.1	8.6	9.2
high-spin	2045.9	2045.6	2045.2	7.3	8.3	8.8
Val67Arg						
low-spin	2024.8	2024.3	2023.7	8.4	8.9	9.4
high-spin	2046.6	2046.2	2045.8	7.3	7.7	8.4
His64Thr						
low-spin	2018.6	2018.2	2018	13.5	14	16.5
high-spin	2046.5	2046.4	2046.3	15.3	17.2	18
His64Lys						
low-spin(I)	2027.1	2026.6	2025.8	8.4	8.9	9.3
low-spin(II)	2021.9	2021.4	2020.8	13	14.3	16.9
high-spin	2046.7	2046.2	2045.8	9	10.4	13.9
His64Ile						
low-spin	2016.7	2016.6	2016.9	14	16.7	19.2
high-spin	2043.6	2043.4	2045.5	14.4	17.6	22.8
	2001.9	2001.5	2001.2	9.9	9.5	10.3
sodium azide	2049	2048.3	2047.4	25.3	25.7	27.2

With increasing temperature, two trends can be observed in the infrared spectra of MbN_3 complexes and of the free azide ion: the ν_{max} shifts to lower energy, and the half-bandwidth increases. It has been shown in earlier studies that ligands bound to the heme iron in proteins exhibit significantly narrower bandwidths than free ligands or ligands bound to iron porphyrins in solution. The smaller bandwidth can be explained by the more ordered nature of the protein-bound ligand and by differences in solvent accessibility and, therefore, changes in solvent polarity (Maxwell & Caughey, 1978; McCoy & Caughey, 1970). The slight increase in half-bandwidth at higher temperatures observed in the myoglobin azide complexes can be attributed to increased mobility (greater disorder) of the bound azide. A slight increase in the half-bandwidth and a shift of the ν_{max} to lower energy were also observed in FTIR studies of MbCO complexes (Balusubramannian et al., 1993).

Figure 2 shows the experimental infrared spectra and the results of curve-fitting for the Val67Arg (Figure 2A) and the Lys45Glu (Figure 2B) variants at 293 K. Both of these variants exhibit infrared absorption spectra similar to that of the wild-type protein in terms of the relative intensities of low-spin and high-spin components and of half-bandwidths. Nevertheless, a small but significant shift in the band maxima of the low-spin bands is observed in both samples. In the Lys45Glu mutant, the band maximum is shifted to lower energy (2022.8 cm^{-1}), whereas in Val67Arg the maximum is shifted to higher energy (2024.3 cm^{-1}). The same tendency is observed at lower (277 K) and higher (313 K) temperature. No significant shift of the absorption band arising from the

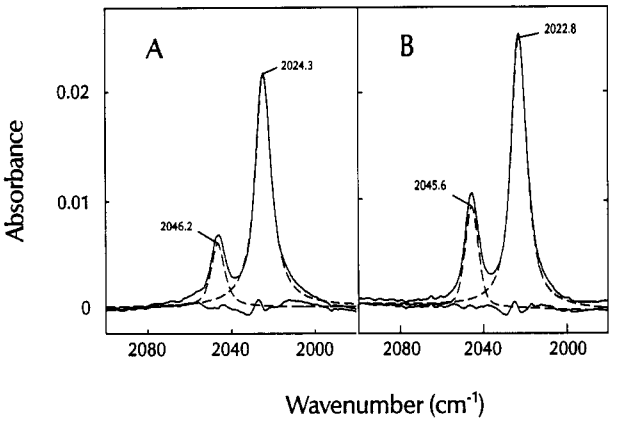

FIGURE 2: Infrared spectra of variant metMbN$_3$ complexes at 293 K: experimental spectra, upper solid lines; absorption bands identified from curve-fitting procedure, dashed lines; residuals (experimental spectrum minus sum of fitted absorption bands), lower solid line. (A) Val67Arg ([Mb], 3.6 mM; [azide], 2.8 mM); (B) Lys45Glu ([Mb], 5 mM; [azide], 3.9 mM).

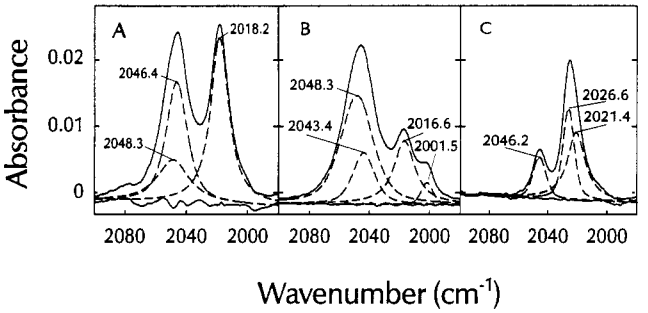

FIGURE 3: Infrared spectra of distal His variant metMbN$_3$ complexes at 293 K: (A) His64Thr ([Mb], 6 mM; [azide], 5 mM); (B) His64Ile ([Mb], 7 mM; [azide], 3.3 mM); (C) His64Lys ([Mb], 5 mM; [azide], 4 mM). Experimental spectra, solid curves; absorption bands identified from curve-fitting procedure, dashed lines; residuals (experimental minus sum of fitted absorption bands), lower solid lines.

high-spin form is found in these samples. A double variant with a second lysyl residue substituted with a glutamyl residue (Lys45Glu/Lys63Glu) shows the same trend as the Lys45Glu variant, namely, a shift of the ν_{max} of the low-spin band to lower energy (see Table 2, spectra not shown).

The infrared absorption spectra (293 K) of the azide complexes formed by the distal histidine variants (His64Thr, His64Lys, His64Ile) are shown in Figure 3. Large differences are observed between the infrared spectra of wild-type and His64 variants. The spectrum of the His64Thr variant (Figure 3A) exhibits a large shift of the MbN$_3$ low-spin band to lower energy (2018.2 cm^{-1}), while the maximum of the band assigned to the high-spin form (2046.4 cm^{-1}) is only slightly shifted. Both bands exhibit significantly greater half-bandwidths than the wild-type MbN$_3$ complex. As this variant has a decreased affinity for azide, some residual free azide is seen in the infrared spectrum, even with an excess of Mb over azide.

The His64Ile variant has a much lower affinity for azide (K_d = 4.2 mM) than do the other Mb variants. Therefore, the FTIR spectrum of His64Ile in the presence of azide (Figure 3B) is dominated by the broad absorption band of the free azide ion at 2048.3 cm^{-1}, which made the curve-fitting for this variant less accurate. The MbN$_3$ low-spin band of His64Ile (2016.6 cm^{-1}) is shifted even more than that for His64Thr and also exhibits a broader bandwidth. The corresponding high-spin band for this variant is found at 2043.4 cm^{-1}. An additional band observed at 2001.5 cm^{-1} is not present in any of the other variants. The origin of this weak band is not yet clear. The decrease of this new band with increasing temperature together with the position of ν_{max} at low energy indicates that it may be produced by a second low-spin form.

The infrared spectrum of the azide complex of the His64Lys (Figure 3C) variant is more complicated because it could not be fitted with just one low- and one high-spin band. In addition to an absorption band at 2026.6 cm^{-1} ($\Delta\nu_{1/2}$ = 8.9 cm^{-1}), another broader band ($\Delta\nu_{1/2}$ = 14.3 cm^{-1}) in the region typical for the low-spin form of MbN$_3$ is found (ν_{max} = 2021.4 cm^{-1}). The absorbance in the region of the high-spin bands was fitted with one absorption band at 2046.2 cm^{-1} ($\Delta\nu_{1/2}$ = 10.4 cm^{-1}). However, the presence of another band produced by another high-spin form (the counterpart to the band at 2021.4 cm^{-1}) cannot be ruled out because it is also possible to fit the absorbance around 2046 cm^{-1} with two bands having similar maxima but different intensities and half-band widths. This possibility must be considered because the maxima of the high-spin absorption bands do not seem to vary significantly from variant to variant. Therefore, even when the absorption maxima of the two low-spin forms are significantly different, two high-spin bands might occur at nearly the same position.

Temperature Dependence of the FTIR Spectra. The infrared spectra of the MbN$_3$ complexes were obtained at three different temperatures. All the variants exhibit a temperature-dependent high-spin/low-spin equilibrium. The equilibrium constant K_s = [N$_3^-$](low-spin)/[N$_3^-$](high-spin) was determined from the integrated areas of the high-spin and low-spin bands. The same transition probabilities are assumed for the high- and low-spin bands because the total area of the absorption bands of bound azide (total area = integrated area of the high-spin band + integrated area of the low-spin band) varies only slightly with temperature (±10%).

The thermodynamic parameters $\Delta H°$ and $\Delta S°$ were estimated from data obtained at three different temperatures by least-squares fit of the data to the Gibbs equation based on a plot of ln K vs $1/T$. The results obtained in this manner are listed and compared with values obtained by other techniques in Table 3.[1] The value of $\Delta H°$ (–3.1 kcal/mol) obtained in the current study of recombinant wild-type Mb is close to the values reported previously for myoglobin obtained from horse heart on the basis of magnetic susceptibility measurements (Beetlestone & George, 1964; Iiuzuka & Kotani, 1969a) and resonance Raman spectroscopy (Tsubaki et al., 1981), but differs from the value obtained by Alben and Fager (1972) by infrared spectroscopy. For the distal histidine mutant His64Thr, a more negative value was obtained (–6.0 kcal/mol), whereas the $\Delta H°$ values for Lys45Glu, Lys45Glu/Lys63Glu, and Val67Arg are intermediate between the values for wild-type Mb and His64Thr.

Iiuzuka and Kotani (1969a,b) determined the thermodynamic parameters for ligand binding to several Mb and Hb derivatives and found that the enthalpy for ligand binding varied in the following sequence: H_2O > N_3 > imidazole. These authors proposed that the $\Delta H°$ values may correlate with the covalency or spectrochemical order of the ligands. Therefore, the change in $\Delta H°$ of the His64Thr variant may be attributable to an increase of covalency relative to that observed for the wild-type protein.

EPR Spectroscopy. The EPR spectra of wild-type and the variant Mbs in the absence of azide are characterized by high-spin EPR signals at pH 7. An exception is the His64Lys

[1] For the His64Lys and His64Ile variants, the thermodynamic parameters were not determined because the presence of more than one band in the low-spin region (His64Lys) or high concentrations of unbound azide (His64Ile) made the fitting process less accurate.

Table 3: Thermodynamic Parameters for the MbN_3 Spin Equilibrium[a]

protein	$\Delta H°$ (kcal/mol)	$\Delta S°$ [cal/(mol·deg)]	method	reference
wild-type metMb	−3.2 (6)	−8 (2)	FTIR	this work
metMb	−5.6 (3)	−15 (1)	IR	Alben & Fager (1972)
metMb	−2.7 (4)	−7 (1)	magnetic susceptibility	Beetlestone & George (1964)
sperm whale metMb	−3.7	−9.6	magnetic susceptibility	Iizuka & Kotani (1969a)
sperm whale metMb	−2.9	nd	resonance Raman spectroscopy	Tsubaki et al. (1981)
Lys45Glu	−4.5 (3)	−13 (1)	FTIR	this work
Lys45Glu/Lys63Glu	−4 (1)	−13 (4)	FTIR	this work
Val67Arg	−4.8 (2)	−13.4 (4)	FTIR	this work
His64Thr	−6.0 (3)	−19.8 (9)	FTIR	this work

[a] The uncertainties indicated for parameters determined in this work are calculated from the standard deviations estimated from linear least-squares fits of the data to the van't Hoff equation, so they probably underestimate the true uncertainties. For those cases where no uncertainty is indicated, none was reported in the reference cited.

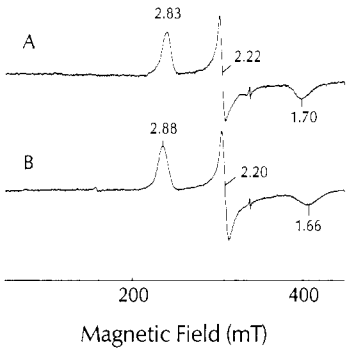

FIGURE 4: X-band EPR spectra (10 K) of $metMbN_3$ complexes ([Mb], 0.8 mM; [azide], 0.2 M; 0.1 M potassium phosphate buffer, pH 7.0): (A) wild-type Mb; (B) His64Thr variant. Instrument settings: 0.63-mW microwave power, 9.45-GHz microwave frequency, 100-kHz modulation frequency, and 1-mT modulation amplitude.

mutant, which shows small amounts of a low-spin form in addition to the major high-spin signal (unpublished data). We assume that the lysine at the distal site can partially ligate to the heme iron and produce a His93–Lys64 coordination environment for the heme iron. This assumption is based upon similarities in the EPR g values to those observed for a semisynthetic cytochrome c possessing an ornithine/histidine ligation (R. Bogumil, C. Wallace, and A. G. Mauk, unpublished results) and to the g values of the alkaline form of cytochrome c (Ferrer et al., 1993).

The azide complexes of wild-type Mb and the variants were studied by EPR spectroscopy at low temperatures (10 K). At this temperature, the MbN_3 complexes are almost completely in the low-spin ground state as reported for the wild-type protein (Iizuka & Kotani, 1969a). The EPR spectra of the azide complexes of recombinant wild-type Mb and the His64Thr variant shown in Figure 4 are characteristic of low-spin heme proteins. No residual ferric high-spin signals of native Mb are seen in these spectra. The sharp signal around $g = 2$ is due to a small amount of a radical, which has been found in some of the recombinant Mb preparations. The g values obtained for the azide complexes of wild-type myoglobin and the variants are virtually identical to each other (data not shown). The EPR parameters of the recombinant wild-type protein ($g_z = 2.83$, $g_y = 2.22$, $g_x = 1.70$) are similar to those obtained with the azide derivatives of commercial horse heart Mb and sperm whale Mb (Sono & Dawson, 1982).

For most of the variants, the g values are quite similar to those exhibited by wild-type myoglobin. However, changes are observed in the g values in the EPR spectrum of the His64Thr (Figure 4) variant. Low-spin EPR spectra of heme proteins are readily analyzed in terms of a distorted octahedral, low-spin $(t_{2g})^5$ complex. The ground state of this configuration is a Kramers doublet that arises from a positive hole occupying the $d_{xy,yz,xz}$ orbitals, which are subject to low-symmetry crystal field distortions, axial (Δ) and rhombic (V), and to spin–orbit coupling (λ). The two crystal field parameters derived (Taylor, 1977) from the experimental g values produce slightly lower values of the rhombic parameter (V) for the His64Thr variant ($V/\lambda = 2.13$) compared to that obtained for wild-type Mb ($V/\lambda = 2.29$), whereas the axial parameter is only slightly affected by the mutation (His64Thr, $\Delta/\lambda = 4.59$; wild-type Mb, $\Delta/\lambda = 4.62$).

Molecular Modeling. The spatial relationship of substituted residues to the heme iron binding site is particularly relevant to the azide binding properties of these proteins. To address this concern, structural models of the variants studied here were obtained by initial fittings on the original structural framework of the wild-type Mb followed by energy minimization calculations. Models of the mutant proteins did not lead to major structural displacements, with the root mean square (rms) deviations of main chain atoms between the energy-minimized models and the wild-type structure being 0.43, 0.47, and 0.41 Å for the Val67Arg, Lys45Glu, and Lys45Glu/Lys63Glu models, respectively. If the experimentally determined pK_a values for histidine residues (Cocco et al., 1992) are used in these calculations, the corresponding rms deviations are 0.42 (Val67Arg), 0.49 (His45Glu), and 0.40 Å (Lys45Glu/Lys63Glu).

The distal heme pocket of wild-type Mb is shown in Figure 5A. The modeled conformations of surface residues substituted in this study are shown in Figure 5B–D. Also shown in Figure 5 is the modeled position of the bound azide anion in each case. The placement of this group was based on the results of an earlier X-ray difference Fourier analysis (Stryer et al., 1964) and model complexes (Dori & Ziola, 1973). On this basis, the azide anion was positioned assuming a Fe–N1–N2 bond angle of 111° and a heme iron to N1 nitrogen atom bond length of 2.1 Å. Distances of the heme iron atom and the N1 nitrogen atom of the bound azide to the charged atoms of residues substituted in the three Mb variants studied are listed in Table 4. In all three protein variants, the N1 nitrogen atom is found to be the closest to these charged groups.

DISCUSSION

The only high-resolution structure of a MbN_3 complex that has been reported at present is that for *Aplysia limacina* myoglobin (Mattevi et al., 1991). The structure of this complex, however, is of limited usefulness to the present study for several reasons. First, the active site of *Aplysia* Mb lacks the distal His64 (E7) residue. Second, the azide bound to the heme iron is oriented toward the surface-exposed portion of the distal site crevice. This azide orientation is stabilized by Arg66 (E10), which assumes a surface orientation in the aquomet form of this protein and is directed into the distal

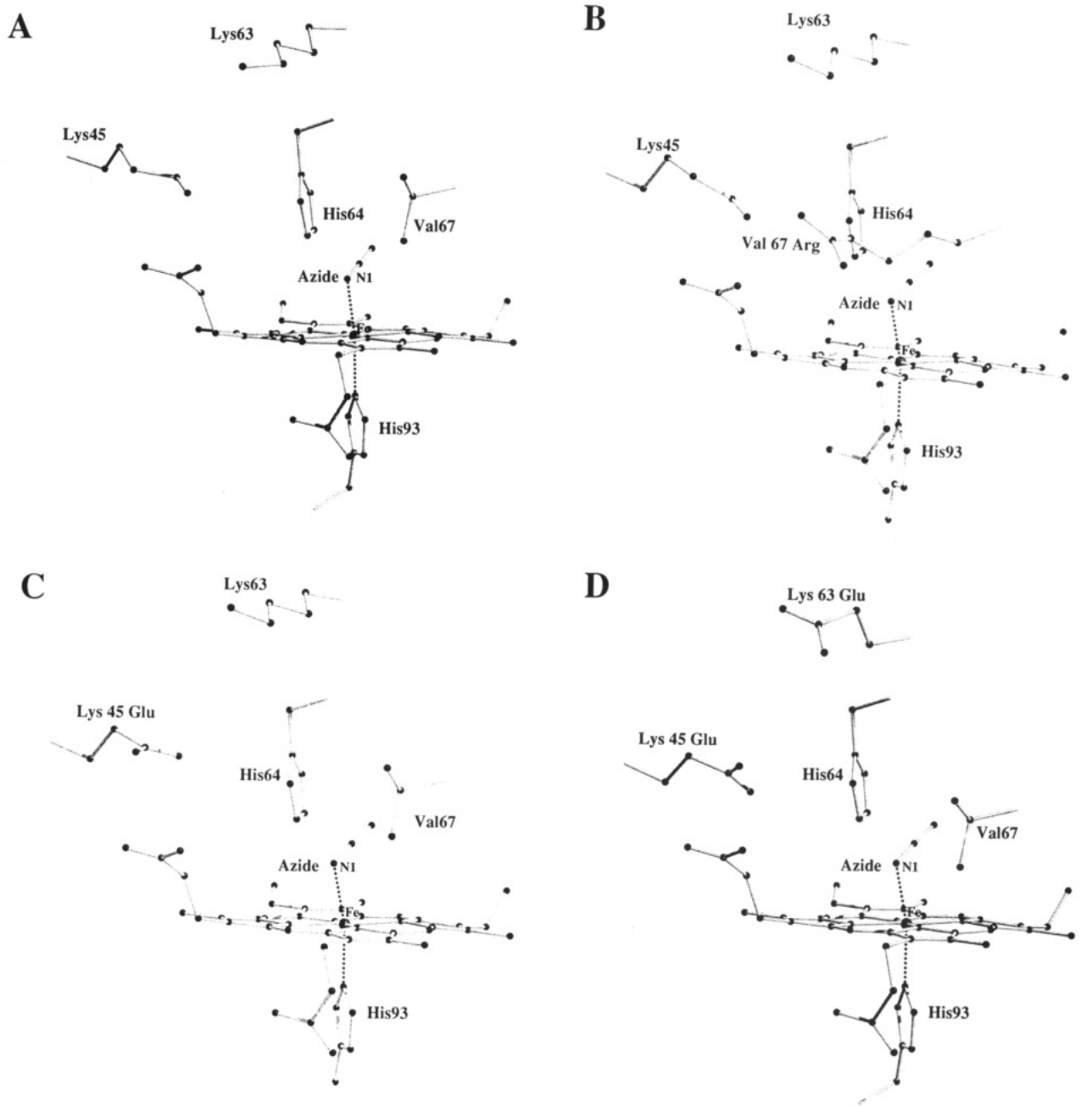

FIGURE 5: Modeled conformations of bound azide and heme binding pocket residues in azide complexes of (A) recombinant wild-type Mb and the (B) Val67Arg, (C) Lys45Glu, and (D) Lys45Glu/Lys63Glu variants of the protein.

pocket in the presence of anionic ligands (Qin et al., 1992; Conti et al., 1993). The similarity of the infrared spectra of the azide complexes of sperm whale and horse heart Mb (Alben & Fager, 1972) indicates that the conformation of azide binding to these two species of protein is nearly identical and supports the use of the earlier results of Stryer (1964) to assist in development of the current models.

Stryer and co-workers (Stryer et al., 1964) originally proposed that a hydrogen bond forms between His64 and the N1 nitrogen of bound azide in sperm whale Mb. The presence of this interaction was later questioned by McCoy and Caughey (1969) because neither the frequencies nor the relative intensities of the infrared bands of the bound azide were significantly dependent on pH over the range 3–11.6 nor were these bands affected by exchange of H_2O for D_2O. Nonetheless, the proximity of His64 to the bound azide leads to the expectation that replacement of this residue should have a significant effect on azide binding. Similarly, smaller effects are anticipated upon replacement of Lys45, Lys63, and Val67 as these residues are further removed from the ligand binding site.

Effect of Charged Residues on Azide Binding. The FTIR spectra of the azide complexes of the Val67Arg, Lys45Glu, and Lys45Glu/Lys63Glu variants are quite similar to the spectrum of the wild-type MbN_3 complex in terms of ν_{max}, half-bandwidth, and high-spin/low-spin equilibrium. Hence, the same binding conformation of the azide anion can be assumed for these variants as occurs in wild-type protein.

The small changes observed in the infrared spectra and the changes in equilibrium binding constants can therefore be analyzed solely as resulting from the introduction of charged residues near the distal heme pocket. The 5–fold decrease of the azide affinity of the Lys45Glu variant and the 5-fold increase of the affinity for the Val67Arg variant are consistent with this assumption. That is, the introduction of a positive charge (Val67Arg) stabilizes the anionic azide ligand, whereas

Table 4: Distances (Å) from the Heme Atom (Fe) to the Bound Azide Nitrogen Atom (N1) and to the Charged Side Chain Atom (R) in Three Modeled Mb Variants

charged group (R)	R–Fe distance[a]	R–azide N1 distance[a]
Val67Arg		
NH1	10.2 (10.3)	9.4 (9.5)
NH2	9.8 (9.7)	9.4 (9.2)
Lys45Glu		
OE1	10.5 (10.4)	9.3 (9.5)
OE2	8.8 (8.8)	7.3 (7.7)
Lys45Glu/Lys63Glu		
Glu45 OE1	9.8 (10.1)	8.4 (8.5)
Glu45 OE2	8.8 (8.6)	6.9 (6.9)
Glu63 OE1	15.3 (15.8)	13.8 (13.9)
Glu63 OE2	14.7 (15.2)	13.4 (13.4)

[a] The values indicated in parentheses are those produced when the experimentally observed pK_a values for histidine residues were used in the modeling calculations.

the negatively charged glutamic acid (Lys45Glu) destabilizes azide binding. The double mutant Lys45Glu/Lys63Glu, which has a 13-fold lower azide affinity than the wild-type protein, follows this same trend.

The effect seen in the infrared spectra of these variants (shift of the ν_{max} of the low-spin azide infrared bands) is opposite for Lys45Glu and Val67Arg. With Lys45Glu, the band is slightly shifted to lower energy (2022.8 cm^{-1} vs 2023.2 cm^{-1} for wild-type Mb), whereas for the Val67Arg variant it is shifted to higher energy (2024.3 cm^{-1}). These shifts are small, but the same trend was observed at all three temperatures measured. The double mutant Lys45Glu/Lys63Glu, with an additional negative charge, shows a shift of the low-spin infrared band similar to that seen for the single mutant Lys45Glu.

If the assumption that the shift of ν_{max} arises from the interaction of charge with the transition dipole moment of the intra-azide bonds is correct, these shifts should correlate with the distance between the charged residues and the bound azide. The estimated distances between the introduced charge carrying side chains in the Lys45Glu and Val67Arg variants and the N1 of the bound azide are in the range of 7.3–9.4 Å, whereas this distance is ~13.5 Å in the case of Glu63 in the Lys45Glu/Lys63Glu variant. The large distance in this case presumably explains why there is no additional shift of ν_{max} in the Lys45Glu/Lys63Glu double mutant over that observed for the Lys45Glu variant. On the other hand, the positively charged side chain of the distal histidine variant (His64Lys) should be the closest to the azide ligand. One of the low-spin bands in the infrared spectrum of this variant is shifted in the same direction as the corresponding band in the Val67Arg variant and is found at the highest energy (2026.6 cm^{-1}) observed. This shift is also likely to result from the positive charge on Lys64 although several factors must be considered in interpretation of the more complex FTIR spectra of the His64 variants. Notably, however, a recent FTIR analysis of the MbCO complexes formed by a large number of sperm whale and pig myoglobin variants indicated that the major factor governing ν_{CO} is the electrostatic potential surrounding the bound ligand and not steric hindrance (Li et al., 1994).

Effect of Substitution of the Distal Histidine. Several spectroscopic studies have shown that replacement of the distal histidine of Mb with larger nonpolar residues (His64Phe, His64Leu, His64Val, His64Met) leads to pentacoordinated ferric heme proteins lacking a water molecule coordinated as the sixth ligand at the distal site (Morikis et al., 1990; Ikeda-Saito et al., 1992; Biram et al., 1993). This finding was recently confirmed by a high-resolution structural study of several His64 variants of sperm whale myoglobin (Quillin et al., 1993). The loss of this bound water molecule is mainly attributable to two factors: the additional hydrophobicity of the nonpolar residues substituted and the disruption of the stabilizing hydrogen bond between the distal hydrogen and the coordinated water molecule. The ferric forms of both the His64Ile variant and the His64Thr variant also seem to be five-coordinated at neutral pH based on their spectroscopic properties (blue-shift of the Soret band and rhombic EPR spectra; data not shown).

The replacement of the distal histidyl residue with nonpolar residues dramatically decreases the affinity for azide binding. For the His64Val and His64Leu variants of human Mb, dissociation constants of 1.1 and 1.4 mM are reported, respectively (Ikeda-Saito et al., 1992). These values are in the same range as the value of 4.2 mM, which we found for the His64Ile variant. The His64Thr mutant exhibits an equilibrium binding constant of 0.44 mM, which is intermediate between the values observed for wild-type Mb and the His64Ile variant. The FTIR spectra of all three distal histidine variants are significantly different from the wild-type MbN_3 spectrum. For both the His64Thr and His64Ile variants, the absorption band of the low-spin form is shifted to significantly lower energy, 2018.6 and 2016.7 cm^{-1}, respectively, and the bandwidths are much greater. The increase in half-bandwidth indicates a greater mobility of the bound azide in these two variants relative to the wild-type protein.

There are several factors which can affect the ν_{max} of the infrared band of the bound azide, the most fundamental of which is a change in bond-order. The large difference in ν_{max} between the high-spin and low-spin azide bands can be explained by an increase of the Fe–nitrogen bond-order (concomitant with a decrease in the bond-order of the intra-azide bands) in the more covalent low-spin form (Alben & Fager, 1972). Thus, the shift observed in the His64Thr and His64Ile spectra may indicate a greater covalent character for azide binding to these variants. The change in the temperature dependence of the spin equilibrium (more negative $\Delta H°$ value for His64Thr) compared to the wild-type protein supports this possibility. However, other factors such as the Fe–N1–N2 bond angle and the inequivalence of the N–N bonds in the azide molecule also affect ν_{max}. The azide ion is generally presumed to be linear and symmetric, possessing equal N–N distances which average 1.15 Å (Dori & Ziola, 1973). On the other hand, in covalent azides and in azido complexes with metal ions, the two N–N distances can be different.[2] Some attempt has been made to relate the degree of asymmetry within the azide to the asymmetric intra-azide stretching frequency. Agrell (1971) found that the greater the differences between the two azide distances the greater the antisymmetric intra-azide stretch, but exceptions to this generalization have been noted subsequently (Dori & Ziola, 1973; Pate et al., 1989).

The angle between the ferric heme iron and the N1 and N2 atoms of the azide molecule can also influence the frequency of the asymmetric azide stretch. In the case of MbCO complexes, the angle between the CO and the heme normal was found to correlate with the stretching frequency of CO (Ormos et al., 1988). However, in the case of the azide complexes studied here, a change in the bond angle seems to be unlikely, because the value found for this angle (111°) in the X-ray structure reported by Stryer (1964) is similar to the

[2] In cases where the azide is asymmetric, the long N–N distance always occurs between the central nitrogen atom and the coordinated nitrogen atom (Dori & Ziola, 1978).

corresponding values for azido complexes of metal ions in which the angle varies between 117° and 132° (Dori & Ziola, 1973). No steric constraints of the type suggested for MbCO complexes appear to be present in MbN_3 complexes.

With the His64Lys variant, two absorption bands assigned to low-spin forms could be resolved, while in all other variants only one major low-spin band is found. The infrared band at 2021.4 cm^{-1} observed for the His64Lys variant has a broad half-bandwidth that is similar to that observed for the low-spin bands of the other distal histidine variants. It is significant that all three distal histidine variants give rise to broader absorption bands than the wild-type protein or the other variants. This supports the existence of direct interaction between the bound azide and the distal His residue, possibly through hydrogen bonding. Such an interaction would increase the equilibrium binding constant and hold the azide ligand in a more ordered conformation that would result in narrower infrared bands. The absence of any change in the infrared spectrum of the MbN_3 complex upon substituting H_2O with D_2O (McCoy & Caughey, 1969) does not rule out hydrogen bonding because in the case of MbCN complexes there is NMR evidence for hydrogen bonding of the distal histidine to cyanide (Cutnell et al., 1981; Lecomte & LaMar, 1987) but no detectable effect of H_2O exchange with D_2O on the infrared spectrum (Yoshikawa et al., 1985).

The His64Lys variant also exhibits a low-spin band (2026.6 cm^{-1}) with a line width similar to that seen for wild-type Mb. This band presumably results from an active-site conformer of the variant in which the substituted lysyl residue assumes a position similar to that occupied by the distal His64 residue normally present. In this position, presumably a hydrogen bond can form with the bound azide. Thus, the broad low-spin band may correspond to a conformer of this variant in which the lysine is oriented away from the azide to allow greater space in the heme pocket for azide motion and broadening of the corresponding infrared absorption band while the sharp low-spin band corresponds to a conformer in which the range of azide motion is restricted by hydrogen bonding to Lys64.

In *Aplysia* Mb, which lacks a distal histidine and has an arginine at position 66 (E10), a hydrogen bond forms between bound azide and this arginine side chain (Conti et al., 1993). In an attempt to model the active site of *Aplysia* Mb in sperm whale Mb, the distal His64 was replaced by valine, and Thr67 (E10) was replaced by an arginine (Cutrozzola et al., 1991; Allocatelli et al., 1993). It was observed that the increase in the azide dissociation constant determined for the His64Val variant can be substantially counterbalanced by the additional Thr67Arg substitution, which was proposed to stabilize azide binding through formation of a hydrogen bond with the bound azide ligand. The azide equilibrium dissociation rate in our His64Lys variant is only 4 times greater than that of wild-type Mb and much lower than that of the other distal histidine variants, supporting the possibility of hydrogen bonding between Lys64 and azide in horse heart myoglobin.

The present study establishes that the infrared absorption properties of coordinated azide are particularly useful in detecting electronic and structural perturbations produced by modifications of the distal heme pocket of myoglobin. On the other hand, the electronic and EPR spectra of the variant MbN_3 complexes studied here are relatively insensitive to the conformation of the bound azide or to changes in the distal heme pocket. The general validity of this latter characteristic is currently the subject of further study.

ACKNOWLEDGMENT

We thank Dr. David Thackray for helpful discussions and Terry Lo for assistance with the molecular modeling calculations.

REFERENCES

Adachi, S., Sunohari, N., Ishimori, K., & Morishima, I. (1992) *J. Biol. Chem. 267*, 12614–12621.

Adachi, S., Nagano, S., Ishimori, K., Watanabe, Y., & Morishima, I. (1993) *Biochemistry 32*, 241–252.

Agrell, I. (1971) *Acta Chem. Scand.*, 2965–2974.

Alben, J. O., & Fager, L. Y. (1972) *Biochemistry 11*, 842–847.

Allocatelli, C. T., Cutrozzola, F., Brancaccio, A., Brunori, M., Quin, J., & La Mar, G. N. (1993) *Biochemistry 32*, 6041–6049.

Balasubramanian, S., Lambright, D. G., & Boxer, S. G. (1993) *Proc. Natl. Acad. Sci. U.S.A. 90*, 4718–4722.

Beetlestone, J., & George, P. (1964) *Biochemistry 3*, 707–714.

Biram, D., Garatt, C. J., & Hester, R. E. (1993) *Biochim. Biophys. Acta 1163*, 67–74.

Braunstein, D., Ansari, A., Berendsen, J., Cowen, B. R., Egeberg, K. D., Frauenfelder, H., Hong, M. K., Ormos, P., Sauke, T. B., Scholl, R., Schulte, A., Sligar, S. G., Springer, B. A., Steinbach, P. J., & Young, R. D. (1988) *Proc. Natl. Acad. Sci. U.S.A. 85*, 8497–8501.

Carver, T. E., Rohlfs, R. J., Olson, J. S., Gibson, Q. H., Blackmore, R. S., Springer, B. A., & Sligar, S. G. (1990) *J. Biol. Chem. 265*, 20007–20020.

Cocco, M. J., Kao, Y.-H., Phillips, A. T., & Lecomte, T. J. (1992) *Biochemistry 31*, 6481–6491.

Conti, E., Moser, C., Rizzi, M., Mattevi, A., Lionetti, C., Coda, A., Ascendi, P., Brunori, M., & Bolognesi, M. (1993) *J. Mol. Biol. 233*, 498–508.

Cutnell, J. D., La Mar, G. N., & Kong, S. B. (1981) *J. Am. Chem. Soc. 103*, 3567–3572.

Cutruzzola, F., Allocatelli, C. T., Ascenzi, P., Bolognesi, M., Sligar, S. G., & Brunori, M. (1991) *FEBS Lett. 282*, 281–284.

Dori, Z., & Ziola, R. F. (1973) *Chem. Rev. 73*, 247–254.

Egeberg, K. D., Springer, B. A., Martinis, S. A., & Sligar, S. G. (1990) *Biochemistry 29*, 9783–9791.

Evans, S. V., & Brayer, G. D. (1988) *J. Biol. Chem. 263*, 4263–4268.

Evans, S. V., & Brayer, G. D. (1990) *J. Mol. Biol. 213*, 885–897.

Ferrer, J. C., Guillemette, G., Bogumil, R., Inglis, S. C., Smith, M., & Mauk, A. G. (1993) *J. Am. Chem. Soc. 115*, 7507–7508.

Guillemette, G. J., Matsushima-Hibiya, Y., Atkinson, T., & Smith, M. (1991) *Protein Eng. 4*, 585–592.

Iizuka, T., & Kotani, M. (1968) *Biochim. Biophys. Acta 154*, 417–419.

Iizuka, T., & Kotani, M. (1969a) *Biochim. Biophys. Acta 181*, 275–286.

Iizuka, T., & Kotani, M. (1969b) *Biochim. Biophys. Acta 194*, 351–363.

Ikeda-Saito, M., Hori, H., Andersson, L. A., Prince, R. C., Pickering, I. J., George, G. N., Sanders, C. R., Lutz, R. S., McKelvey, E. J., & Mattera, R. (1992) *J. Biol. Chem. 267*, 22843–22852.

Lecomte, J. T., & La Mar, G. N. (1987) *J. Am. Chem. Soc. 109*, 7219–7220.

Li, T., Quillin, M. L., Phillips, G. N., Jr., & Olson, J. S. (1994) *Biochemistry 33*, 1433–1446.

Magliozzo, R. S., & Peisach, J. (1993) *Biochemistry 32*, 8446–8456.

Mattevi, A., Gatti, G., Coda, A., Rizzi, M., Ascendi, P., Brunori, M., & Bolognesi, M. (1991) *J. Mol. Recogn. 4*, 1–6.

Maxwell, J. C., & Caughey, W. S. (1978) *Methods Enzymol. 54*, 302–323.

McCoy, S., & Caughey, W. S. (1970) *Biochemistry 9*, 2387–2393.

Morikis, D., Champion, P. M., Springer, B. A., Egeberg, K. D., & Sligar, S. G. (1990) *J. Biol. Chem. 265*, 12143–12145.

Ormos, P., Braunstein, D., Frauenfelder, H., Hong, M. K., Lin, S.-L., Sauke, T. B., & Young, R. D. (1988) *Proc. Natl. Acad. Sci. U.S.A. 85*, 8492–8496.

Pate, J. E., Ross, P. K., Thamann, T. J., Reed, C. A., Karlin, K. D., Sorell, T. N., & Solomon, E. I. (1989) *J. Am. Chem. Soc. 111*, 5198–5209.

Qin, J., La Mar, G., Ascoli, F., Bolognesi, M., & Brunori, M. (1992) *J. Mol. Biol. 224*, 891–897.

Quillin, M. L., Arduini, R. M., Olson, J. S., & Phillips, G. N., Jr. (1993) *J. Mol. Biol. 234*, 140–155.

Rohlfs, R. J., Mathew, A. J., Carver, T. E., Olson, J. S., Springer, B. A., Egeberg, K. D., & Sligar, S. G. (1990) *J. Biol. Chem. 265*, 3168–3176.

Sono, M., & Dawson, J. H. (1982) *J. Biol. Chem. 257*, 5496–5502.

Springer, B. A., Egeberg, K. D., Sligar, S. G., Rohlfs, R. J., Mathews, A. J., & Olson, J. S. (1989) *J. Biol. Chem. 264*, 3057–3060.

Stryer, L., Kendrew, J. C., & Watson, H. C. (1964) *J. Mol. Biol. 8*, 96–104.

Taylor, C. P. S. (1977) *Biochim. Biophys. Acta 491*, 137–149.

Tsubaki, M., Srivastave, R. B., & Yu, N.-T. (1981) *Biochemistry 20*, 946–952.

Yoshikawa, S., O'Keeffe, D. O., & Caughey, W. S. (1985) *J. Biol. Chem. 260*, 3518–3528.